Article

Effect of Pressure, H$_2$/CO Ratio and Reduction Conditions on Co–Mn/CNT Bimetallic Catalyst Performance in Fischer–Tropsch Reaction

Omid Akbarzadeh [1],*, **Noor Asmawati Mohd Zabidi** [2], **Guangxin Wang** [3], **Amir Kordijazi** [4], **Hamed Sadabadi** [5], **Seyedehmaryam Moosavi** [1], **Arman Amani Babadi** [6], **Nor Aliya Hamizi** [1], **Yasmin Abdul Wahab** [1], **Marlinda Ab Rahman** [1], **Suresh Sagadevan** [1], **Zaira Zaman Chowdhury** [1] **and Mohd Rafie Johan** [1]

1   Nanotechnology & Catalysis Research Centre, University of Malaya, Kuala Lumpur 50603, Malaysia; m.moosavi1987@gmail.com (S.M.); aliyahamizi@um.edu.my (N.A.H.); yasminaw@um.edu.my (Y.A.W.); marlinda@um.edu.my (M.A.R.); sureshsagadevan@gmail.com (S.S.); dr.zaira.chowdhury@um.edu.my (Z.Z.C.); mrafiej@um.edu.my (M.R.J.)
2   Department of Fundamental and Applied Sciences, Universiti Teknologi PETRONAS, Bandar Seri Iskandar, Perak 32610, Malaysia; noorasmawati_mzabidi@utp.edu.my
3   Research Center for High Purity Materials, Henan University of Science and Technology, Luoyang 471023, China; wgx58@126.com
4   Department of Industrial and Manufacturing Engineering, University of Wisconsin Milwaukee, Milwaukee, WI 53211, USA; kordija2@uwm.edu
5   School of Metallurgy and Materials Engineering, Collage of Engineering, University of Tehran, Tehran 1417466191, Iran; hamed.sadabadi@ut.ac.ir
6   Functional Omics and Bioprocess Development Laboratory, Institute of Biological Sciences, Faculty of Science, University of Malaya, Kuala Lumpur 50603, Malaysia; ar.amani65@gmail.com
*   Correspondence: omid.akbarzadeh63@gmail.com or omid@um.edu.my; Tel.: +60-135853522

check for updates

Abstract: The effects of process conditions on Fischer–Tropsch Synthesis (FTS) product distributions were studied using a fixed-bed microreactor and a Co–Mn/CNT catalyst. Cobalt and Manganese, supported on Carbon Nanotubes (CNT) catalyst were prepared by a Strong Electrostatic Adsorption (SEA) method. CNT supports were initially acid and thermally treated in order to functionalize support to uptake more Co clusters. Catalyst samples were characterized by Transmitted Electron Microscope (TEM), particle size analyzer, and Thermal Gravimetric Analysis (TGA). TEM images showed catalyst metal particle intake on CNT support with different Co and Mn loading percentage. Performance test of Co–Mn/CNT in Fischer–Tropsch synthesis (FTS) was carried out in a fixed-bed micro-reactor at different pressures (from 1 atm to 25 atm), H2/CO ratio (0.5–2.5), and reduction temperature and duration. The reactor was connected to the online Gas Chromatograph (GC) for product analysis. It was found that the reaction conditions have the dominant effect on product selectivity. Cobalt catalyst supported on acid and thermal pre-treated CNT at optimum reaction condition resulted in CO conversion of 58.7% and C5+ selectivity of 59.1%.

Keywords: carbon nanotubes; heterogenous catalysis; thermal treatment; cobalt-manganese; Fischer–Tropsch; bimetallic catalyst; acid treatment; gas process

1. Introduction

Fischer–Tropsch synthesis (FTS) uses syngas to produce hydrocarbons and plays an important role in all eco-friendly fuels and renewable energy resources. The gas to liquid process is attractive because

of abundant natural gas and coal reserves, which can be used as feed sources rather than terminating crude oil reserves. Fuels synthesized with the FTS method is heterogenous catalysis, environmentally friendly, and has low sulfur and aromatic ring content [1]. Using a cobalt catalyst is common choice of catalyst for FTS [2]. Liquid hydrocarbons, i.e., those with five carbon atoms and above, referred to as C5+ are of most economic interest. Therefore, optimizing the reaction product distribution is crucial, and it is influenced by operating conditions such as temperature, pressure, the ratio of H2/CO, type of reactor and the catalyst, etc. [3–7]. The increase in operating pressure for FT reaction over cobalt-based catalysts has been reported to have an insignificant effect or to increase the reaction rate and C5+ selectivity [8]. It has been reported that the selectivity to low molecular hydrocarbons is increased with the increase of reaction temperature and inlet H2/CO ratio, while the selectivity to high molecular hydrocarbons is increased with the decrease of total pressure [9]. Some investigators reported the effect of operation parameters on the product distribution from cobalt-based catalysts [9–11] and showed that the olefin contents of the product spectrum decreased with increasing pressure, which was consistent with previous investigations [12,13]. This work is a continuation of the same project which has previously been investigated and published. Previous works focused on catalyst preparation variables such as effects of catalyst active site confinement in CNT channels, addition of Mn to Co/CNT catalyst, acid and thermal treatment of CNT support, catalyst pH, percentage of Cobalt catalyst loading, calcination condition and catalyst particle size [14–17]. The present study aims to prepare a CNT-supported cobalt manganese bimetallic catalyst using the SEA method and focus on the study of the effect of Fischer–Tropsch reaction parameters such as pressure, H2/CO ratio, and reduction conditions on the performance of Co–Mn/CNT bimetallic catalyst.

2. Experimental

2.1. Carbon Nanotube Support Functionalization

Functionalization and activation of CNT using nitric acid are important prior to metal loading [18]. Purpose of the functionalization process was to improve the interaction between foreign molecules and the surface of CNT. Acid pretreatment purifies pristine CNT, introduces oxygen-containing groups (-OH) onto the surface, and helps to open closed caps of CNT [19]. The most widely accepted approach for activation and functionalization of carbon nanotubes is through a wet chemical oxidation process. Approximately 2 g of commercial CNT (purity > 95%, CVD, length: 10–20 µm, diameter: 30–50 nm, Nanostructured & Amorphous Materials Inc., Houston, TX, USA) (denoted as, as-received CNT) added into a single-necked round-bottom flask was functionalized and activated with 35 vol% nitric acid (Merck) at 110 °C for 10 h [20]. A conventional reflux system, consisting of the single-necked round-bottom flask with a thermometer, condenser, and oil bath, was used. After refluxing, the mixture was cooled to room temperature, diluted with deionized water, filtered through a 0.2 µm pore-sized filter membrane, and washed several times until the pH of the filtrate was approximately 7 [21]. The neutralized slurry dried in an oven overnight at 120 °C and the acid-treated CNT were thermally treated at 900 °C in flowing argon at 20 mL min^{-1} [22]. In the present study, CNT support samples with acid and thermal treatment were designated CNT.A.T.

2.2. Determination of PZC, Catalyst Uptake on CNT Support and Catalyst Synthesis

Conventional impregnations method used for synthesizing cobalt catalyst yielded heterogeneously dispersion of cobalt particles on the CNT support, but the Strong Electrostatic Adsorption (SEA) method, based on the electrostatic attraction of oppositely charged particles, resulted in a higher catalyst active sites dispersion and narrower distribution [23–26]. Silica, Alumina, CNT, and metal oxides have hydroxyl groups on their surface. In the SEA method, the point of zero charges (PZC) is a pH value of medium at which hydroxyl group on the surface remain neutral. In the case of pH<PZC, hydroxyl group will protonate, so they have positive charged and therefore attract anions. Where pH>PZC hydroxyl groups will deprotonate and become negatively charged and adsorbing cations. A series of

experiments to determined noble metals supported on CNT by using cationic hexamine of complexes of noble metal showed that metal uptake increase significantly at pH>PZC [23,25,26]. All samples prepared via SEA, at optimum pH, were found to be a smaller size and better dispersion in comparison to those prepared by the conventional impregnation method. Equilibrium pH at high oxide loading (EpHL) method [27] was employed to determine the PZC of CNT support. Solutions at pH values in the range of 2–14 were prepared by adding nitric acid or ammonium hydroxide into distilled water. Amount of 50 mL of each solution were added into 0.5 g CNT in a conical flask. The mixture was shaken for 1 h using a rotary shaker prior to measurement of final pH value. Plateau in final pH versus initial pH plot as shown in Figure 1a indicates PZC of CNT was found to be 9.5.
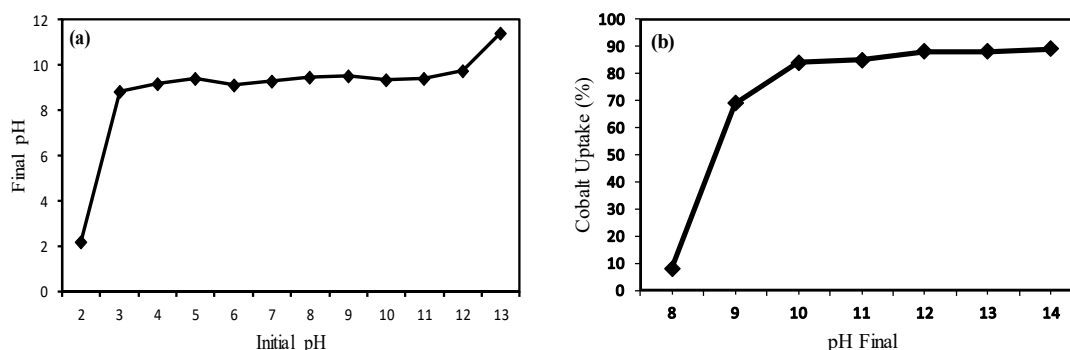

Figure 1. Determination of (**a**) PZC of CNT support, (**b**) Co–Mn uptake versus pH survey by AAS.

The pH of the cobalt nitrate precursor solution was adjusted to a range of 2–14 to perform cobalt uptake versus pH survey. Weighed 0.5 g CNT were added in solutions and measured after 1 h shaken for final pH. An amount of 5 mL of filtered cobalt solution for each sample was tested by atomic absorption spectrophotometer (AAS) for cobalt content. Figure 1b shows a plot of cobalt uptake versus pH and the optimum pH indicated for cobalt uptake is 14. At selected pH = 14, the cobalt precursor was adsorbed by 10 wt% at Co–Mn metal loads from an excess solution on CNT support (to prevent pH shift). The sample was filtered and dried for 24 h under air flow. The dried sample was calcined to remove residual reactants in a tubular furnace at 400 °C for 4 h under air flow. All catalysts were prepared using a powerful method of electrostatic adsorption (SEA) with a total metal load of 10 wt%. Total metal loading of 10 wt% (Co and Mn) divided between Co and Mn with following percentage codding, Co/CNT, 95Co5Mn/CNT, 90Co10Mn/CNT, 85Co15Mn/CNT, 80Co20Mn/CNT.

2.3. Catalyst Characterization and Equations

FT catalyst performance is strongly influenced by catalyst physicochemical properties, and therefore, it is essential to characterize these properties. FTS catalyst properties needing classification are chemical and physical surface properties, reducibility of catalysts, catalytic activity and selectivity. This work is continuation of the same project which is previously investigated and published. In the previous studies X-Ray Diffraction (XRD), Brunauer–Emmett–Teller (BET), X-ray Photoelectron Spectroscopy (XPS), etc characterization preformed and discussed [14–17]. Characterization techniques performed for FTS catalysts include Transmission electron microscopy (TEM) analysis on a Zeiss LIBRA 200 FE TEM at 200 kV accelerating voltage. Figure 2 showing TEM images of different Co-Mn/CNT bimetallic catalyst formulation.

Scanning electron microscopy (FESEM-EDX) (Zeiss Supra 55 VP, accelerating voltage: 5 KV, magnification: 100.00 KX and working distance: 4 mm) was used to analyze morphology and surface elemental composition of samples. Figure 3 showing FESEM images of different Co-Mn/CNT bimetallic catalyst formulation.
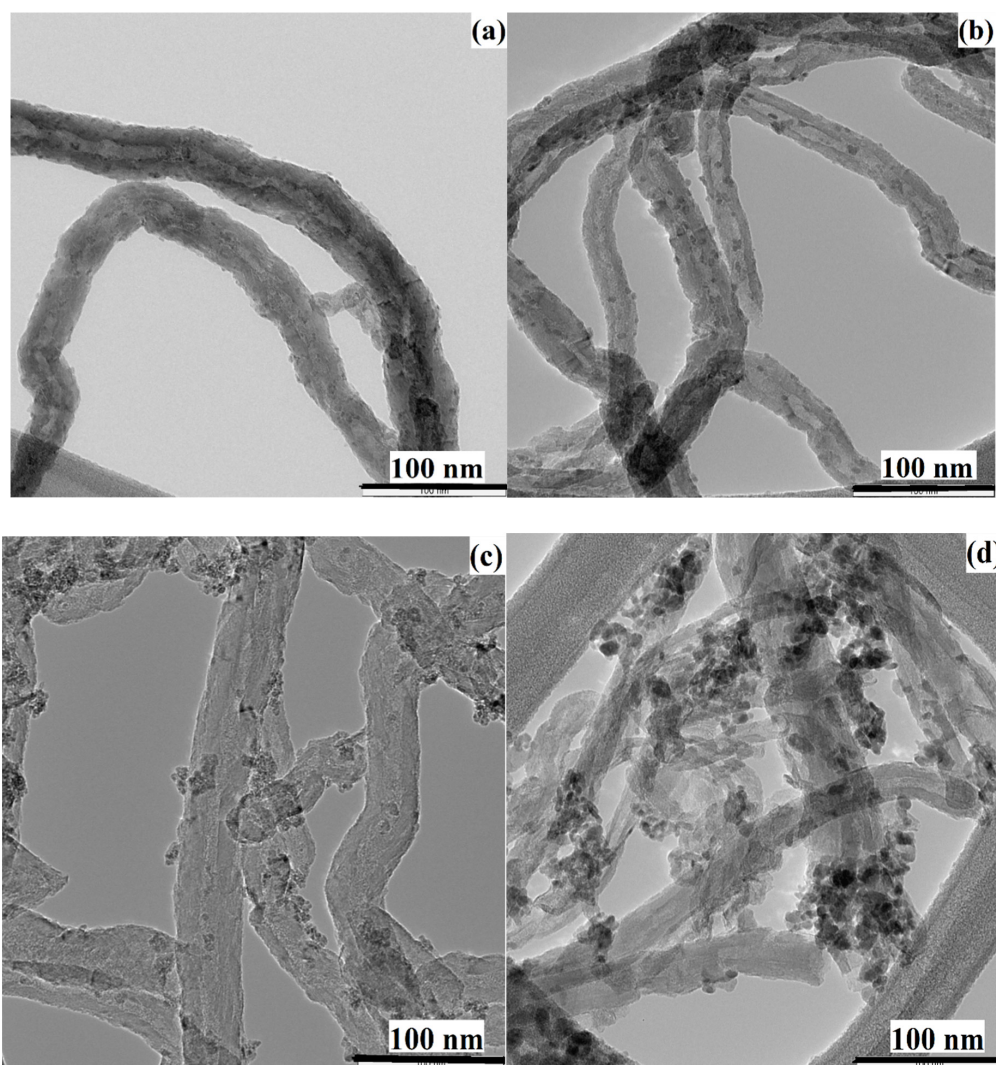
Figure 2. TEM images of (**a**) 95Co5Mn/CNT, (**b**) 90Co10Mn/CNT, (**c**) 85Co15Mn/CNT, (**d**) 80Co20Mn/CNT catalysts.

Flame atomic absorption spectrometer (AAS) by Agilent Technologies GTA 120 was employed to measure Co and Mn uptake on CNT support in an air-acetylene flame [28,29].

$$\% \; Reduction = \frac{O_2 \; Uptake \times \frac{2}{3} \times \text{Atomic Weight}}{Percent \; Metal} \tag{1}$$

where:

O_2-uptake = μmol/g.cat of O_2 calculated from TPO spectra of catalyst.

Atomic weight = MW of metal

% Metal = weight percentage of metal in catalyst.

$$\% \; \text{Dispersion} = \frac{\frac{\text{H}_2\text{uptake} \times \text{atomic weight} \times \text{stoichiometry}}{\% \; \text{metal}}}{(\text{total Co})} \\ = \frac{\text{number of Co atoms on the surface}}{\text{total number of Co atoms in the sample}} \times 100 \tag{2}$$

where:

H_2-uptake = amount of H_2 consumed in mmol/g. cat calculated from the peak area of H_2-TPD spectra

Atomic weight = MW of metal

% Metal = weight percentage of metal in catalyst.

Stoichiometry = 2

A number of active sites of catalysts were calculated using % dispersion and % reduction calculated using Equation (3) [30].

$$No.\ of\ active\ sites = \frac{wt\ of\ Co\ in\ the\ sample \times reduction \times dispersion \times N_A}{MW} \qquad (3)$$

where:

N_A = Avogadro's number

MW = atomic weight of metal.

$$H_2\ uptake \left(\frac{moles}{gcat}\right) = \frac{the\ analytical\ area\ from\ TPD \times calibration\ value}{sample\ weight \times 24.5} \qquad (4)$$

$$O_2\ uptake\ (moles/gcat) = \frac{the\ sum\ of\ consumed\ pulse\ areas \times calibration\ value}{sample\ weight \times 24.5} \qquad (5)$$
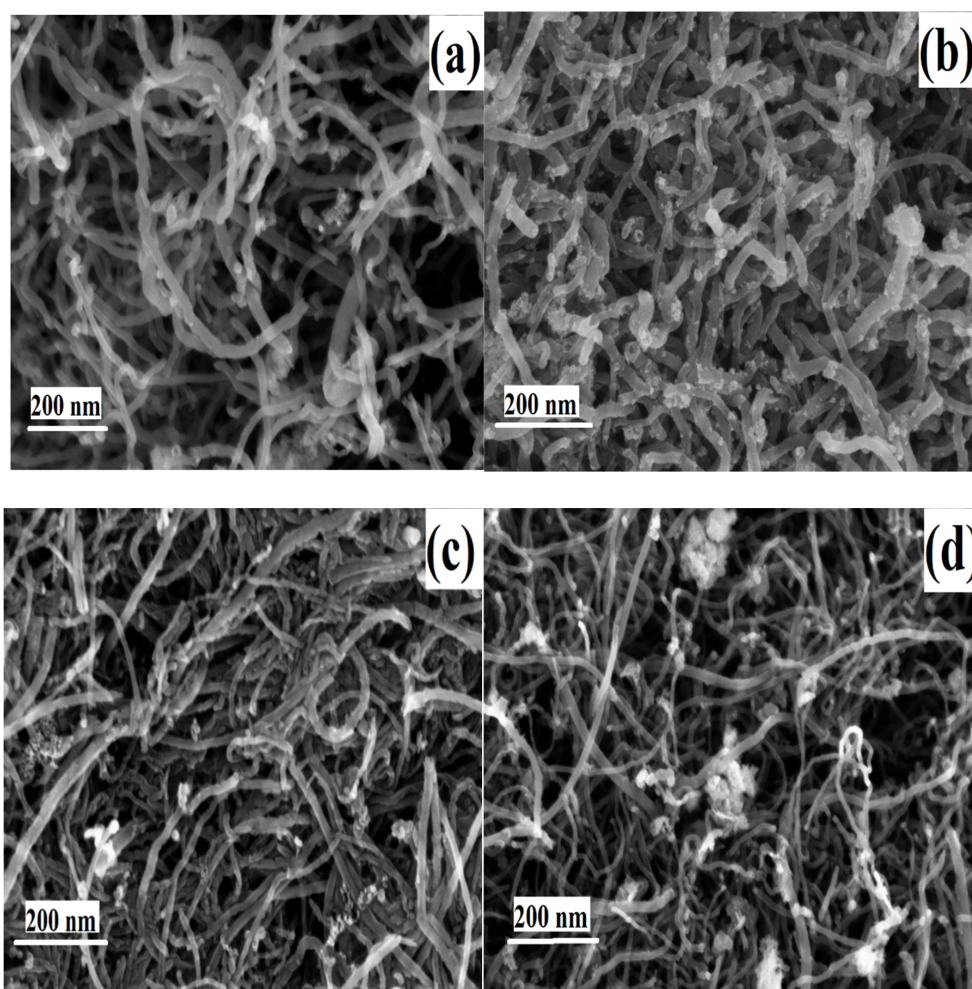

Figure 3. SEM images of (**a**) 95Co5Mn/CNT, (**b**) 90Co10Mn/CNT, (**c**) 85Co15Mn/CNT, (**d**) 80Co20Mn/CNT catalysts.

2.4. Microreactor Setup, Sampling, and Composition Analysis

Microactivity-reference equipment (Micromeritics) was used to study the performance of nanocatalyst in Fischer–Tropsch (FT) reaction. An online gas chromatograph (Agilent Hewlett-Packard Series 6890, USA) equipped with a TCD detecting CO_2, O_2, N_2, and CO and FID detecting (Agilent J&W DB-5 column) detecting Methane, Ethane, Ethylene, Acetylene, Propane, iso-Butane, n-Butane, n-Pentane, n-Hexane, and n-Heptane were used to analyze the gaseous product.

Percentage of conversion for CO and selectivity of methane (CH_4) and C5+ was calculated using Equations (6)–(8), respectively [30].

$$CO\ conversion\ (\%) = \frac{CO_{in} - CO_{out}}{CO_{in}} \times 100 \tag{6}$$

where:

CO_{in} = Mole % of CO feeding to the reactor from mass fellow meter.

CO_{out} = Mole % of CO exit from the reactor and detect with GC.

$$CH_4\ selectivity\ (\%) = \frac{S_{CH_4}}{T_{HC}} \times 100 \tag{7}$$

where:

S_{CH_4} = Mole of CH_4 detected by GC

T_{HC} = Total moles of hydrocarbons detected by GC

$$C_{5+} selectivity\ (\%) = \frac{S_{C5+}}{T_{HC}} \times 100 \tag{8}$$

where:

S_{C5+} = Mole of C_{5+} detected by GC

T_{HC} = Total moles of hydrocarbons detected by GC

Fischer–Tropsch synthesis rate (RFTS) shown in Equation (9) and water gas shift reaction rate (RWGS) shown in Equation (10), is equivalent to the formation rate of carbon dioxide (RFCO2) and can be defined by [31–33]:

$$RFTS\ (g\ HC/g\ cat/h) = g\ hydrocarbons\ produced/g\ cat * h^{-1} \tag{9}$$

$$RWGS\ (g\ CO_2/g\ cat/h) = RFCO_2 = g\ CO_2\ produced/g\ cat * h^{-1} \tag{10}$$

3. Process Studies

It is important to reduce and activate calcined catalysts before an FTS reaction. Catalysts were activated under the H2, 1.8 L/h flow at 420 °C for 12.5 h in the reactor tube. Reactor temperature was cooled down to the desired reaction temperature after catalyst activation in-situ and flushed with helium for 10 min. This study was conducted to investigate the effects of the H2/CO (v/v) reaction ratio (0.5/1, 1/1, 1.5/1, 2/1 and 2.5/1), pressure (1, 5, 10, 15, 20, 25 atm) and different reduction temperature and duration on the performance of different CNT catalysts. Effects on the catalytic performance of monometallic and bimetallic Co–Mn nanocatalysts, such as reaction pressure, H2/CO feed gas molar ratios and reduction condition were studied. The results of the reaction were compared in terms of CO conversion and selectivity of the product. For the process study portion, all reactions were conducted three times and the standard deviation value was ±1 percent for all reactions. Figure 4 showed a reactor schematic (Microactivity-reference device, Micromeritics) used for FTS reactions.
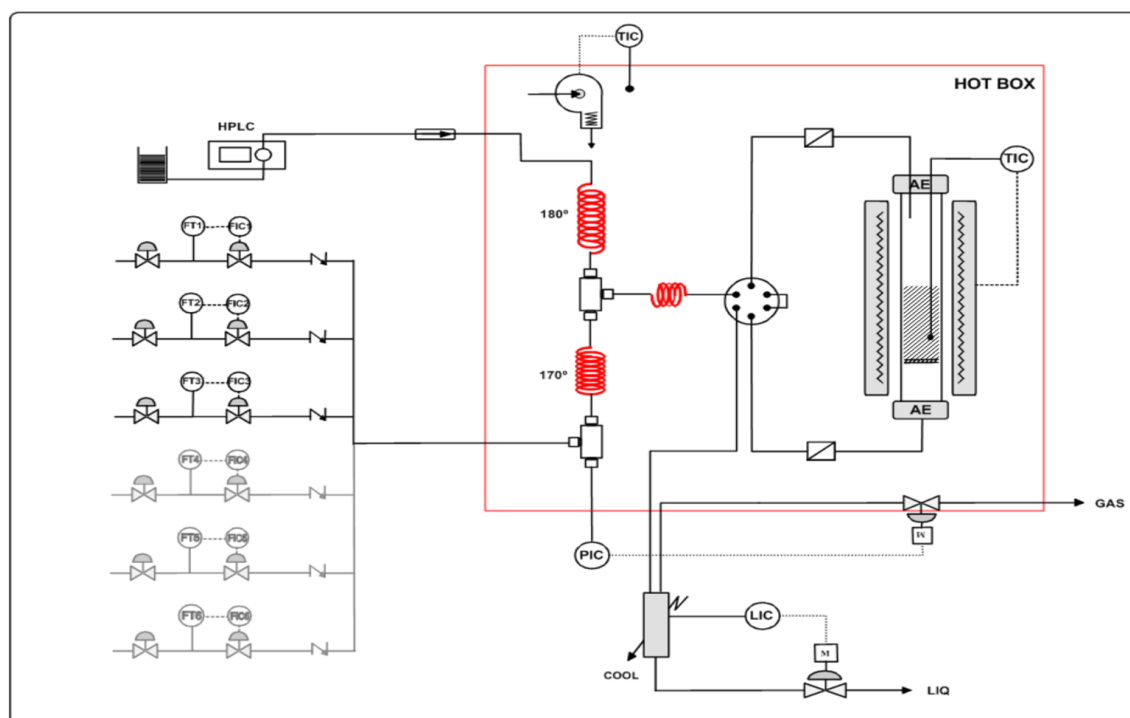
Figure 4. Schematic of the reactor (Microactivity-reference equipment, Micromeritics).

3.1. Effect of Pressure on Catalytic Performance

Table 1 shows the CO conversion dependence with an increase in total operating pressure. It has been observed that CO conversion also increases with an increase in operating pressure from 1 to 25 atm. CO conversion was increased to 89.4% for the 95Co5Mn/CNT catalyst at 20 atm operating pressure and the trend was reported [9]. It was suggested that increased operating pressure increased the concentration of reactant species over active catalyst sites, and, hence, increased CO conversion and was attributed to increased adsorption of CO molecules on the catalyst surface and improved chances of the collision of reactants and catalysts [9].

The effect of operating pressure on the selectivity of C1 and C2–C4 over selected catalysts is shown in Table 1. With operating pressure increasing from 1 to 25 atm, methane selectivity decreased to 15 percent over the Co–Mn/CNT catalyst. Mukenz (Mukenz 2010) [34] suggested that the rate of formation of methane depends on the operating pressure. Li and colleagues [35] observed that methane selectivity was suppressed by an increase in operating pressure. An increase in FTS operating pressure has been suggested to alert partial reactant or product pressure resulting in methane selectivity depression. As shown in Table 1, increased pressure to 25 atm resulted in increased selectivity of C5+ hydrocarbons. This effect was more significant for catalysts with 95Co5Mn/CNT where C5+ selectivity increased to 85.8%. The results indicated that with increased operating pressure, there is an increased chain growth probability and thus favored higher hydrocarbon selectivity [30]. It was also suggested that increased operating pressure increased chain propagation of CHx monomers to the active catalyst surface, and thus increased selectivity for higher hydrocarbons [36]. Bergr et al. and Farias et al. reported a similar effect, discovering that with increased operating pressure there was a significant increase in chain growth probabilities [37,38].

Table 1. Effect of reaction pressure (atm) on CO conversion and catalyst selectivity.

CO Conversion	1	5	10	15	20	25
Co/CNT	32.2	50.4	53.7	55.6	58.7	61.5
95Co5Mn/CNT	49.4	78.5	81.7	84.4	86.6	89.5
90Co10Mn/CNT	44.6	75.8	77.0	78.1	79.8	83.9
85Co15Mn/CNT	42.2	68.6	70.1	72.2	73.2	77.7
80Co20Mn/CNT	38.9	58.1	62.6	64.9	66.3	68.2
C_1 Selectivity						
Co/CNT	16.6	15.2	14.5	13.8	9.5	12.7
95Co5Mn/CNT	15.5	13.2	12.4	11.9	11.8	6.1
90Co10Mn/CNT	14.1	13.7	12.2	11.4	8.3	11.3
85Co15Mn/CNT	14.7	14.1	13.1	12.3	9.1	11.4
80Co20Mn/CNT	15.1	14.6	13.8	13.2	10.0	12.1
C_2–C_4 selectivity						
Co/CNT	42.1	33.6	30.6	25.6	13.4	21.8
95Co5Mn/CNT	26.2	16.3	11.3	8.6	6.7	6.5
90Co10Mn/CNT	32.7	25.8	20.5	15.4	8.4	9.3
85Co15Mn/CNT	37.5	30.7	26.7	21.3	9.4	13.6
80Co20Mn/CNT	41.5	35.2	31.4	25.5	10.5	18.1
C_{5+} selectivity						
Co/CNT	27.3	36.2	39.5	45.4	59.1	50.5
95Co5Mn/CNT	55.3	66.7	72.3	76.1	81.5	76.3
90Co10Mn/CNT	48.2	56.2	62.3	68.2	78.0	74.6
85Co15Mn/CNT	43.3	50.2	55.2	61.4	76.5	70.7
80Co20Mn/CNT	38.4	45.2	49.8	56.5	74.5	64.8

3.2. Effects of H2/CO Feed Ratio on Catalytic Performance

For the constant weight of the catalyst, five different H2/CO feed ratios (H2/CO = 0.5, 1, 1.5, 2 and 2.5) were used at 240 °C. Table 2 summarizes the effects of the H2/CO feed ratio on CO conversion over bimetallic and monometallic Co–Mn nanocatalysts (at P = 20 atm, T = 240 °C and 3 L/g.h. space velocity). Conversion of CO increased to a feed ratio of 2 for monometallic Co/CNT and then decreased as the H2/CO ratio increased to 2.5. An increase in H2/CO feed ratios increased partial H2 pressure and consequently increased CO conversion [39]. The decrease in CO conversion for H2/CO feed ratios below 2 may be due to a decrease in H2 partial pressure leaving some CO molecules unhydrogenated. The H2/CO ratio higher than 2, increase partial H2 pressure and therefore decrease activity. H. Schulz et al. research groups have also reported similar trends [40]. Reducing the H2/CO ratio from 2 to 1 reduced the percentage of CO conversion for the Co/CNT catalyst sample from 64.3% to 46.7%. Decreasing the H2/CO ratio will reduce the partial pressure of syngas on the gas phase resulting in a reduction in the amount of CO adsorbed on the surface of the catalyst. Decreasing the rate of FTS can be explained by the kinetic rate equation of cobalt-based FTS catalysts with partial CO pressure in denominator [41]. A similar trend was observed for bimetallic systems to that of monometallic Co, where CO conversion increased from 62.6% to 80.5% with an increased H2/CO feed ratio of 1 to 2, passing through an optimum H2/CO ratio of 2. These CO conversion trends at different H2/CO feed ratios were consistent with various literature reports [40,41].

Table 2 summarizes the effects of different H2/CO feed ratios on C1 and C2–C4 selectivity. Increased selectivity for methane based on increasing the H2/CO feed ratio from 0.5 to 2.5 for monometallic Co and bimetallic catalyst. An increase in H2/CO feed ratio increased H2 partial pressure which would have increased CO hydrogenation and consequently decreased methane selectivity [39]. As the feed ratio of H2/CO increases further, more H2 will be adsorbed on the surface of the catalyst, thus reducing CO adsorption. The effects of different H2/CO feed ratios on C5+ catalyst selectivity are shown in Table 2. Increasing H2/CO feed ratios for Co catalyst increased C5+ selectivity for 95Co5Mn/CNT

bimetallic catalyst from 50.6% to 81.5%. Increasing the feed ratio of H2/CO has been suggested to decrease the partial CO pressure on Co-based catalysts resulting in increased hydrocarbon chain propagation and thus increased selectivity for higher hydrocarbons [39]. A similar trend followed by bimetallic Co–Mn/CNT as that of Monometallic Co. The increasing partial CO pressure on the catalyst surface increases the amount of adsorbed CO and increases the growth of the chain and decreases the termination reaction to paraffin.

Table 2. Effect of H2/CO ratio on CO conversion and catalyst selectivities.

CO Conversion	0.5	1	1.5	2	2.5
Co/CNT	25.6	46.7	53.3	58.7	55.8
95Co5Mn/CNT	41.7	62.6	69.7	86.6	74.7
90Co10Mn/CNT	36.6	57.3	65.6	79.8	70.5
85Co15Mn/CNT	33.8	52.8	59.8	73.2	65.3
80Co20Mn/CNT	28.3	49.7	56.9	66.3	61.7
C_1 selectivity					
Co/CNT	16.5	16.0	15.5	9.5	14.3
95Co5Mn/CNT	13.5	13.1	12.5	11.8	11.3
90Co10Mn/CNT	14.5	14.0	13.5	13.3	12.2
85Co15Mn/CNT	15.5	15.0	14.5	14.1	13.3
80Co20Mn/CNT	16.4	15.5	15.1	15.0	13.7
C_2–C_4 selectivity					
Co/CNT	45.7	33.7	26.5	13.4	28.8
95Co5Mn/CNT	35.6	23.6	15.5	6.7	4.4
90Co10Mn/CNT	38.8	29.8	21.5	8.4	9.6
85Co15Mn/CNT	42.6	33.8	24.5	9.4	13.7
80Co20Mn/CNT	45.5	35.5	29.6	10.5	16.5
C_{5+} selectivity					
Co/CNT	30.2	41.3	48.8	59.1	54.5
95Co5Mn/CNT	50.6	64.4	72.7	81.5	78.1
90Co10Mn/CNT	45.7	57.8	65.6	78.0	76.5
85Co15Mn/CNT	42.3	52.6	61.3	76.5	71.5
80Co20Mn/CNT	38.9	49.2	56.8	74.5	67.5

3.3. Effect of Reduction Time Period and Temperature on Catalytic Performance

The sample was reduced at 420 °C by flowing 25 mL/min, H2 gas before starting the FTS reaction. Metal oxide converts to active metals in the reduction part and activates sites by the catalyst [42]. Variety of reduction time from 3 to 15 h and temperature at 350, 400, 450 and 500 °C at 240 °C reaction temperature, 20 atm pressure, 20 mg catalyst mass; flow rate: 30 mL/min H2 and 15 mL/min CO (H2/CO ratio: 2).

In the FTS process, Table 3 indicates that CO conversion increased from 21.5% to about 65.7% with an increase in the reduction period from 3 to 15 h due to a higher fraction of metallic Co which forms active support sites. In contrast, the effect of the reduction period on C1 and C2–C4 selectivity increased from 15.2% to 21.6% with an increase in the reduction period from 3 to 15 h C1 and from 70.8% to 24.2% for all catalysts for C2 to C4. Increasing the reduction period from 3 to 15 h leads to an increase in C5+ selectivity for the 95Co5Mn/CNT catalyst from 25.4% to 86.1%. Table 4 shows that increasing temperature reduction from 340 to 420 °C, CO conversion of 95Co5Mn/CNT catalyst increased from 46.6% to 81.4% due to the desired temperature on CNT support to active cobalt sites. However, due to sintering and agglomeration of metal active sites, reduction temperature increased from 340 to 500 °C and CO conversion declined.

Table 3. Effect of reduction time (h) on CO conversion and catalyst selectivities.

CO Conversion	3	6	9	12	15
Co/CNT	21.5	35.7	46.2	58.7	58.8
95Co5Mn/CNT	30.4	67.9	83.1	86.6	86.7
90Co10Mn/CNT	28.9	65.7	70.5	83.8	83.8
85Co15Mn/CNT	25.7	52.6	60.6	73.2	73.3
80Co20Mn/CNT	23.9	48.7	52.8	66.3	66.5
C_1 selectivity					
Co/CNT	16.2	14.1	11.7	9.5	9.6
95Co5Mn/CNT	17.3	15.6	13.9	11.8	11.7
90Co10Mn/CNT	19.6	17.7	15.6	13.3	13.4
85Co15Mn/CNT	21.8	19.9	17.4	14.1	14.5
80Co20Mn/CNT	23.7	20.4	17.7	15.0	15.4
C_2–C_4 selectivity					
Co/CNT	70.8	65.6	34.4	13.4	13.5
95Co5Mn/CNT	60.6	48.8	27.9	6.7	6.8
90Co10Mn/CNT	63.5	52.7	29.7	8.4	8.5
85Co15Mn/CNT	66.9	55.6	33.9	9.4	9.5
80Co20Mn/CNT	69.6	57.4	37.6	10.5	10.6
C_{5+} selectivity					
Co/CNT	15.3	30.3	35.7	59.1	59.3
95Co5Mn/CNT	25.4	34.2	40.6	81.5	81.5
90Co10Mn/CNT	23.9	31.6	37.3	78.0	78.2
85Co15Mn/CNT	21.7	29.8	35.1	76.5	76.6
80Co20Mn/CNT	18.6	26.4	32.6	74.5	74.7

Table 4. Effect of reduction temperature (°C) on CO conversion and catalyst selectivity.

CO Conversion	340	380	420	460	500
Co/CNT	31.4	40.8	58.7	37.7	29.4
95Co5Mn/CNT	46.6	62.6	86.6	56.9	43.6
90Co10Mn/CNT	45.7	58.7	79.8	52.8	40.7
85Co15Mn/CNT	37.6	51.8	73.2	47.7	35.9
80Co20Mn/CNT	35.8	46.6	66.3	42.4	32.5
C_1 selectivity					
Co/CNT	25.5	22.3	9.5	20.7	29.4
95Co5Mn/CNT	15.3	12.7	11.8	12.6	18.7
90Co10Mn/CNT	18.6	15.9	13.3	14.7	20.6
85Co15Mn/CNT	21.9	17.4	14.1	16.6	23.4
80Co20Mn/CNT	22.4	19.5	15.0	18.4	26.3
C_2–C_4 selectivity					
Co/CNT	40.4	37.2	13.4	40.2	41.9
95Co5Mn/CNT	37.5	33.3	6.7	31.7	38.6
90Co10Mn/CNT	38.6	35.4	8.4	34.8	39.4
85Co15Mn/CNT	41.7	38.6	9.4	37.9	40.5
80Co20Mn/CNT	42.2	38.8	10.5	38.6	40.2
C_{5+} selectivity					
Co/CNT	30.5	41.3	59.1	40.7	30.7
95Co5Mn/CNT	42.9	55.5	81.5	57.4	44.3
90Co10Mn/CNT	39.4	50.6	78.0	52.6	41.7
85Co15Mn/CNT	35.6	45.8	76.5	47.5	37.1
80Co20Mn/CNT	32.5	43.4	74.5	44.8	34.4

For 95Co5Mn/CNT bimetallic catalyst, the selectivity of C1 and C2–C4 follows the same general trend. Increasing temperature reduction from 340 to 420 °C leads to a decrease in C1 selectivity from 15.3% to 8.4% and from C1 selectivity from 420 to 500 °C from 8.4% to 18.7%. Increasing temperature reduction from 340 to 420 °C, the selectivity of C5+ increased from 42.9% to 85.8% and increased temperature reduction from 420 to 500 °C, the selectivity of C5+ decreased from 85.8% to 44.3% [43,44].

3.4. Characterization of Spent Catalyst

Figure 5 shows TEM images of 95Co5Mn/CNT.A.T600 and 95Co5Mn/CNT.A.T900 catalyst samples that spent 10 h at 240 °C and shows increased growth of cobalt particles on CNT support. Figure 5 shows TEM images of spent catalysts at 95Co5Mn/CNT where thermal treatment at (a) 600 and (b) 900 °C were conducted. Catalyst particle size increased from 4.2 to 20.5 nm for CNT thermal samples pretreated at 600 °C and increased from 7.2 to 14.1 nm for CNT thermal samples pretreated at 900 °C; indicating a catalyst sintering phenomena. The deactivation step showed significantly high sintering during FTS. Results of the TEM test show that the sintering rate of particles on the outer surfaces of CNT is higher than that of particles inside the CNT channels.
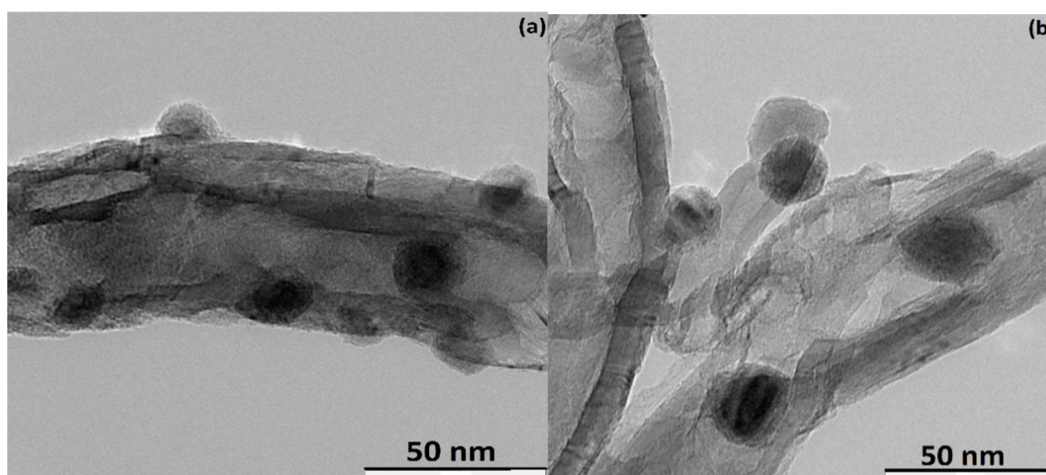

Figure 5. TEM image of (**a**) 95Co5Mn/CNT.A.T600 and (**b**) 95Co5Mn/CNT.A.T900 after 10 h reaction.

4. Conclusions

The bimetallic Co–Mn catalyst was prepared using the SEA method on functionalized CNT support. Acid and thermal CNT pretreatment were conducted for functionalization of CNT support. The performance of the CNT-supported Co–Mn catalyst was tested in the FTS reaction. Co–Mn/CNT catalyst has high activity and C5+ selectivity and is stable. It also concluded that variables of reaction conditions have a significant impact during the FTS process on catalytic activity and product selectivity. Study of reaction conditions showed (with an increased pressure from 1 to 20 atm) increased CO conversion for 95Co5Mn/CNT catalyst from 49.4% to 89.4%. However, for the 95Co5Mn/CNT catalyst sample, increasing reaction pressure from 1 to 20 atm increased the selectivity of the C5+ product from 55.3 to 85.8%. However, the effect of the H_2/CO (v/v) feed ratio increasing from 0.5 to 2 resulted in an increase for CO conversion of 95Co5Mn/CNT catalyst from 41.7 to 86.6% and for C5+ from 50.6% to 81.5%. The effect of reduction time increasing from 3 to 15 h resulted in an increase for CO conversion of 95Co5Mn/CNT catalyst from 30.4% to 86.7% and for C5+ selectivity from 25.4% to 81.5%. A reduction temperature increase from 340 to 460 °C resulted an increase for CO conversion of 95Co5Mn/CNT catalyst from 46.6 to 56.9 and for C5+ selectivity from 42.9 to 57.4%. In terms of CO conversion and C5+ product selectivity, the feed ratio of H_2/CO of 2 (v/v), reaction pressure of 20 atm, reduction time of 20 h and reduction temperature of 420 °C were found as optimum values of the Fischer–Tropsch reaction for the 95Co5Mn/CNT catalyst.

References

1. Shokouhimehr, M.; Asl, M.S.; Mazinani, B. Modulated large-pore mesoporous silica as an efficient base catalyst for the Henry reaction. *Res. Chem. Intermed.* **2018**, *44*, 1617–1626. [CrossRef]

2. Iglesia, E. Design, synthesis, and use of cobalt-based Fischer–Tropsch synthesis catalysts. *Appl. Catal. A Gen.* **1997**, *161*, 59–78. [CrossRef]

3. Mirzaei, A.A.; Shirzadi, B.; Atashi, H.; Mansouri, M. Modeling and operating conditions optimization of Fischer–Tropsch synthesis in a fixed-bed reactor. *J. Ind. Eng. Chem.* **2012**, *18*, 1515–1521. [CrossRef]

4. Feyzi, M.; Irandoust, M.; Mirzaei, A.A. Effects of promoters and calcination conditions on the catalytic performance of iron–manganese catalysts for Fischer–Tropsch synthesis. *Fuel Process. Technol.* **2011**, *92*, 1136–1143. [CrossRef]

5. Mirzaei, A.A.; Babaei, A.B.; Galavy, M.; Youssefi, A. A silica supported Fe–Co bimetallic catalyst prepared by the sol/gel technique: Operating conditions, catalytic properties and characterization. *Fuel Process. Technol.* **2010**, *91*, 335–347. [CrossRef]

6. Atashi, H.; Siami, F.; Mirzaei, A.A.; Sarkari, M. Kinetic study of Fischer–Tropsch process on titania-supported cobalt–manganese catalyst. *J. Ind. Eng. Chem.* **2010**, *16*, 952–961. [CrossRef]

7. Júnior, L.C.P.F.; de Miguel, S.; Fierro, J.L.G.; do Carmo Rangel, M. Evaluation of Pd/La2O3 catalysts for dry reforming of methane. In *Studies in Surface Science and Catalysis*; Bellot Noronha, F., Schmal, M., Falabella Sousa-Aguiar, E., Eds.; Elsevier: Amsterdam, The Netherlands, 2007; Volume 167, pp. 499–504.

8. Gheitanchi, R.; Khodadadi, A.A.; Taghizadeh, M.; Mortazavi, Y. Effects of ceria addition and pre-calcination temperature on performance of cobalt catalysts for Fischer–Tropsch synthesis. *React. Kinet. Catal. Lett.* **2006**, *88*, 225–232. [CrossRef]

9. Liu, Y.; Teng, B.-T.; Guo, X.-H.; Li, Y.; Chang, J.; Tian, L.; Hao, X.; Wang, Y.; Xiang, H.-W.; Xu, Y.-Y.; et al. Effect of reaction conditions on the catalytic performance of Fe-Mn catalyst for Fischer–Tropsch synthesis. *J. Mol. Catal. A Chem.* **2007**, *272*, 182–190. [CrossRef]

10. Morales, F.; de Smit, E.; de Groot, F.M.F.; Visser, T.; Weckhuysen, B.M. Effects of manganese oxide promoter on the CO and H2 adsorption properties of titania-supported cobalt Fischer–Tropsch catalysts. *J. Catal.* **2007**, *246*, 91–99. [CrossRef]

11. Zhang, C.-H.; Yang, Y.; Teng, B.-T.; Li, T.-Z.; Zheng, H.-Y.; Xiang, H.-W.; Li, Y.-W. Study of an iron-manganese Fischer–Tropsch synthesis catalyst promoted with copper. *J. Catal.* **2006**, *237*, 405–415. [CrossRef]

12. Arsalanfar, M.; Mirzaei, A.A.; Bozorgzadeh, H.R.; Atashi, H. Effect of process conditions on the surface reaction rates and catalytic performance of MgO supported Fe–Co–Mn catalyst for CO hydrogenation. *J. Ind. Eng. Chem.* **2012**, *18*, 2092–2102. [CrossRef]

13. Kim, S.-M.; Bae, J.W.; Lee, Y.-J.; Jun, K.-W. Effect of CO_2 in the feed stream on the deactivation of Co/γ-Al_2O_3 Fischer–Tropsch catalyst. *Catal. Commun.* **2008**, *9*, 2269–2273. [CrossRef]

14. Akbarzadeh, O.; Mohd Zabidi, N.; Abdul Wahab, Y.; Hamizi, N.; Chowdhury, Z.; Merican Aljunid Merican, Z.; Ab Rahman, M.; Akhter, S.; Rasouli, E.; Johan, M. Effect of Cobalt Catalyst Confinement in Carbon Nanotubes Support on Fischer–Tropsch Synthesis Performance. *Symmetry* **2018**, *10*, 572. [CrossRef]

15. Akbarzadeh, O.; Mohd Zabidi, N.; Hamizi, N.; Abdul Wahab, Y.; Aljunid Merican, Z.; Yehya, W.; Akhter, S.; Shalauddin, M.; Rasouli, E.; Johan, M. Effect of pH, Acid and Thermal Treatment Conditions on Co/CNT Catalyst Performance in Fischer–Tropsch Reaction. *Symmetry* **2019**, *11*, 50. [CrossRef]

16. Akbarzadeh, O.; Mohd Zabidi, N.; Abdul Wahab, Y.; Hamizi, N.; Chowdhury, Z.; Aljunid Merican, Z.; Ab Rahman, M.; Akhter, S.; Shalauddin, M.; Johan, M. Effects of Cobalt Loading, Particle Size, and Calcination Condition on Co/CNT Catalyst Performance in Fischer–Tropsch Reactions. *Symmetry* **2018**, *11*, 7. [CrossRef]

17. Akbarzadeh, O.; Mohd Zabidi, N.A.; Aljunid Merican, Z.M.; Sagadevan, S.; Kordijazi, A.; Das, S.; Amani Babadi, A.; Ab Rahman, M.; Hamizi, N.A.; Abdul Wahab, Y.; et al. Effect of Manganese on Co–Mn/CNT Bimetallic Catalyst Performance in Fischer–Tropsch Reaction. *Symmetry* **2019**, *11*, 1328. [CrossRef]

18. Akbarzadeh, O.; Zabidi, N.A.M.; Abdullah, B.; Subbarao, D. Synthesis and Characterization of Co/CNTs Catalysts Prepared by Strong Electrostatic Adsorption (SEA) Method. *Appl. Mech. Mater.* **2014**, *625*, 328–332. [CrossRef]

19. Akbarzadeh, O.; Zabidi, N.A.M.; Abdullah, B.; Subbarao, D. Dispersion of Co/CNTs via strong electrostatic adsorption method: Thermal treatment effect. *AIP Conf. Proc.* **2015**, *1669*, 020052. [CrossRef]

20. Akbarzadeh, O.; Mohd Zabidi, N.A.; Abdullah, B.; Subbarao, D. Synthesis of Co/CNTs Catalyst via Strong Electrostatic Adsorption: Effect of Calcination Condition. *Adv. Mater. Res.* **2015**, *1109*, 1–5. [CrossRef]

21. Akbarzadeh, O.; Mohd Zabidi, N.A.; Abdullah, B.; Subbarao, D. Synthesis of Co/CNTs via Strong Electrostatic Adsorption: Effect of Metal Loading. *Adv. Mater. Res.* **2014**, *1043*, 101–104. [CrossRef]

22. Akbarzadeh, O.; Mohd Zabidi, N.A.; Abdullah, B.; Subbarao, D. Influence of Acid and Thermal Treatments on Properties of Carbon Nanotubes. *Adv. Mater. Res.* **2013**, *832*, 394–398. [CrossRef]

23. Elbashir, N.O.; Roberts, C.B. Enhanced incorporation of α-olefins in the Fischer–Tropsch synthesis chain-growth process over an alumina-supported cobalt catalyst in near-critical and supercritical hexane media. *Ind. Eng. Chem. Res.* **2005**, *44*, 505–521. [CrossRef]

24. Maitlis, P.M.; Zanotti, V. The role of electrophilic species in the Fischer–Tropsch reaction. *Chem. Commun.* **2009**, 1619–1634. [CrossRef] [PubMed]

25. Dry, M. Chemical concepts used for engineering purposes. *Stud. Surf. Sci. Catal.* **2004**, *152*, 196–257. [CrossRef]

26. Hexana, W.M. A Systematic Study of the Effect of Chemical Promoters on the Precipitated Fe-Based Fischer–Tropsch Synthesis Catalyst. Ph.D. Thesis, Faculty of Science, University of the Witwatersrand, Johannesburg, South Africa, 2009.

27. Park, J.; Regalbuto, J.R. A simple, accurate determination of oxide PZC and the strong buffering effect of oxide surfaces at incipient wetness. *J. Colloid Interface Sci.* **1995**, *175*, 239–252. [CrossRef]

28. Schiavo, D.; Nóbrega, J.A. Interferences in Thermospray Flame Furnace AAS: Co and Mn Behavior. *Spectrosc. Lett.* **2008**, *41*, 354–360. [CrossRef]

29. Tony, K.A.; Kartikeyan, S.; Vijayalakshmy, B.; Prasada Rao, T.; Padmanabha Iyer, C.S. Flow injection on-line preconcentration and flame atomic absorption spectrometric determination of iron, cobalt, nickel, manganese and zinc in sea-water. *Analyst* **1999**, *124*, 191–195. [CrossRef]

30. Zolfaghari, Z.; Tavasoli, A.; Tabyar, S.; Pour, A.N. Enhancement of bimetallic Fe-Mn/CNTs nano catalyst activity and product selectivity using microemulsion technique. *J. Energy Chem.* **2014**, *23*, 57–65. [CrossRef]

31. Jacobs, G.; Das, T.K.; Zhang, Y.; Li, J.; Racoillet, G.; Davis, B.H. Fischer–Tropsch synthesis: Support, loading, and promoter effects on the reducibility of cobalt catalysts. *Appl. Catal. A Gen.* **2002**, *233*, 263–281. [CrossRef]

32. Jacobs, G.; Patterson, P.M.; Das, T.K.; Luo, M.; Davis, B.H. Fischer–Tropsch synthesis: Effect of water on Co/Al$_2$O$_3$ catalysts and XAFS characterization of reoxidation phenomena. *Appl. Catal. A Gen.* **2004**, *270*, 65–76. [CrossRef]

33. Tavasoli, A.; Mortazavi, Y.; Khodadadi, A.A.; Mousavian, M.A.; Sadagiani, K.; Karimi, A. Effects of different loadings of Ru and Re on physico-chemical properties and performance of 15% Co/Al$_2$O$_3$ FTS catalysts. *Iran. J. Chem.* **2005**, *24*, 9–17.

34. Mukenz, T.M. *Graphical Methods for the Representation of the Fischer–Tropsch Reaction: Towards Understanding the Mixed Iron-Cobalt Catalyst Systems*; University of the Witwatersrand: Johannesburg, South Africa, 2010.

35. Li, J.; Jacobs, G.; Das, T.; Zhang, Y.; Davis, B. Fischer–Tropsch synthesis: Effect of water on the catalytic properties of a Co/SiO$_2$ catalyst. *Appl. Catal. A Gen.* **2002**, *236*, 67–76. [CrossRef]

36. De la Pena O'Shea, V.; Alvarez-Galvan, M.; Campos-Martin, J.; Fierro, J. Strong dependence on pressure of the performance of a Co/SiO$_2$ catalyst in Fischer–Tropsch slurry reactor synthesis. *Catal. Lett.* **2005**, *100*, 105–116. [CrossRef]

37. Van Berge, P.; Everson, R. Natural gas conversion IV. *Stud. Surf. Sci. Cat* **1997**, *107*, 207.

38. Fernandes, F.A. Polymerization Kinetics of Fischer-Tropsch Reaction on Iron Based Catalysts and Product Grade Optimization. *Chem. Eng. Technol.* **2005**, *28*, 930–938. [CrossRef]

39. Tristantini, D.; Lögdberg, S.; Gevert, B.; Borg, Ø.; Holmen, A. The effect of synthesis gas composition on the Fischer–Tropsch synthesis over Co/γ-Al$_2$O$_3$ and Co–Re/γ-Al$_2$O$_3$ catalysts. *Fuel Process. Technol.* **2007**, *88*, 643–649. [CrossRef]

40. Schulz, H.; Nie, Z.; Ousmanov, F. Construction of the Fischer–Tropsch regime with cobalt catalysts. *Catal. Today* **2002**, *71*, 351–360. [CrossRef]

41. Yates, I.C.; Satterfield, C.N. Intrinsic kinetics of the Fischer–Tropsch synthesis on a cobalt catalyst. *Energy Fuels* **1991**, *5*, 168–173. [CrossRef]

42. Chetty, R.; Xia, W.; Kundu, S.; Bron, M.; Reinecke, T.; Schuhmann, W.; Muhler, M. Effect of reduction temperature on the preparation and characterization of Pt–Ru nanoparticles on multiwalled carbon nanotubes. *Langmuir* **2009**, *25*, 3853–3860. [CrossRef]

43. Bahome, M.C.; Jewell, L.L.; Hildebrandt, D.; Glasser, D.; Coville, N.J. Fischer–Tropsch synthesis over iron catalysts supported on carbon nanotubes. *Appl. Catal. A Gen.* **2005**, *287*, 60–67. [CrossRef]

44. Graham, U.; Dozier, A.; Khatri, R.; Bahome, M.; Jewell, L.; Mhlanga, S.; Coville, N.; Davis, B. Carbon nanotube docking stations: A new concept in catalysis. *Catal. Lett.* **2009**, *129*, 39–45. [CrossRef]